A three dimensional semi-analytical model for the prediction of gate vibrations immersed in fluid

Tieleman, O. C.; Tsouvalas, A.; Hofland, B.; Peng, Y.; Jonkman, S. N.

DOI
10.1016/j.marstruc.2018.12.007

Publication date
2019

Document Version
Final published version

Published in
Marine Structures

Marine Structures 65 (2019) 134–153

Contents lists available at ScienceDirect

Marine Structures

journal homepage: www.elsevier.com/locate/marstruc

A three dimensional semi-analytical model for the prediction of gate vibrations immersed in fluid

O.C. Tieleman[a,*], A. Tsouvalas[a], B. Hofland[a,b], Y. Peng[a], S.N. Jonkman[a]

[a] Faculty of Civil Engineering and Geosciences, Delft University of Technology, Stevinweg 1, 2628 CN, Delft, the Netherlands
[b] Deltares, Boussinesqweg 1, 2629 HV, Delft, the Netherlands

ARTICLE INFO

Keywords:
Vibrations
Flood gates
Semi-analytical
Coupled modal analysis
Fluid-structure interaction
Wave impacts

ABSTRACT

A model is developed to predict bending vibrations of flood gates with fluid on both sides. The liquid flow is three-dimensional and the gate is represented as a thin plate. The fluid response is considered within the linear potential flow theory including the effect of compressibility and the generation of free surface waves. This way, the hydrodynamic fluid pressure exerted on the gate is predicted accurately in both low and high-frequency regimes. Both the structural and fluid responses are expressed in the modal domain as a superposition of modes. A semi-analytical solution of the fluid-interaction problem is obtained by describing the complete system in terms of in vacuo gate modes, which is computationally efficient compared to existing numerical methods. This allows for the accurate prediction of flood gate vibrations for a large number of simulations, making it possible to perform fatigue calculations and probabilistic evaluations. The case of a typical flat flood gate subjected to an impulsive wave impact is studied with the developed model. Results show the capability of the model to efficiently quantify flood gate vibrations considering the involved fluid-structure interaction, which can lead to more economical designs compared to common engineering practice.

1. Introduction

Flood and lock gates are generally subjected to time-varying loads induced by a variety of sources, such as waves, water flow, earthquakes, wind and tides. Whether these forces lead to significant vibrations, depends on their magnitude and frequency, and the characteristics of the gate-fluid system. The trend to realise gates of increasing scale, contributes to the relevance of taking their dynamic behaviour into consideration from early design stages. A key application in which the dynamic behaviour of gates is relevant, is that of coastal flood gates subjected to wave impacts. These impacts are generally accompanied with high local peak pressures of short duration [1–3].

The magnitude of the dynamic response of a gate does not only depend on the structural characteristics, but is also affected by the interaction with the surrounding fluid [4]. Due to the complexity involved in solving fluid-structure interaction problems, it is common engineering practice to design these gates based on a quasi-static approach in which the effect of the vibrations is accounted for by applying a dynamic amplification factor. The structure is often simplified to a single degree of freedom (SDOF) system [5,6]. Hattori and Tsujioka [7] have performed a series of experiments on the response of elastic plates to wave impacts, and compared the measured response to the theoretical response based on a SDOF system. The dynamic properties of the plate in fluid were experimentally determined. The results show a relatively high discrepancy between measurements of the wall deflection and the prediction

* Corresponding author.
E-mail address: o.c.tieleman@tudelft.nl (O.C. Tieleman).

https://doi.org/10.1016/j.marstruc.2018.12.007
Received 19 September 2018; Received in revised form 17 December 2018; Accepted 28 December 2018
Available online 15 January 2019
0951-8339/

by the single degree-of-freedom model. Although SDOF models yield theoretical insight, they lack the precision to capture the three dimensional vibration behaviour of a gate-fluid system, which significantly limits their applicability as a design instrument. The locality of the peak pressures accompanied with wave impacts complicates the problem further. Currently, vertical breakwaters such as caissons subjected to wave impacts are most commonly designed on the basis of guidelines developed by Goda [8]. Due to their relatively high mass, the dynamic response of caissons is generally reduced compared to the quasi-static consideration. To the authors' knowledge no similar guideline exists for the design of vertical flood gates, such as sluice and sea lock gates. Hence, the formulas of Goda are also used for hydraulic structures at the moment [9,10].

The dynamic behaviour of submerged plates and the involved fluid-structure interaction have been continuously investigated in the past century. Advanced methods to study vibrations influenced by fluid-structure interaction can be divided into three main categories: finite element methods (FEM), boundary element methods (BEM), and (semi)analytical solutions [11]. Lamb [4] was the first to calculate the change in resonance frequency of a thin flexible circular plate extended by an infinite rigid baffle due the presence of incompressible fluid. Many analytical solutions, developed later on, depend on the assumption that the structural modes in the submerged system are approximately the same as the in vacuo modes, which is subscribed to Lamb's work. This will be referred to as the assumed-modes approach. In this case the effect of the surrounding fluid on the respective natural frequencies can be determined by applying hydrodynamic coefficients [12] or the nondimensionalized added virtual mass incremental (NAVMI) factors [13]. Kolkman [14] presents a simple numerical scheme to obtain the added mass coefficient for a given geometry based on incompressible fluid and a null potential at the free surface. Westergaard [15] derived an analytical expression for the hydrodynamic pressures for the situation of a two-dimensional vertical rigid dam adjacent to an infinitely long and wide reservoir with compressible fluid, which is still used in engineering practice. Fu and Price [16] studied the vibration behaviour of partially and totally immersed plates, solving the fluid pressure by employing the Green's function. The vibrational mode shapes of the plate in fluid were considered the same as the in vacuo modes. The effect of the free surface was investigated and shown to have a significant effect on the resonance frequencies. A similar problem was considered by Ergin and Ugurlu [17] in which the in-vacuo dynamic properties of the plate were obtained using standard finite-element software. The fluid response was determined by the use of a boundary integral equation method together with the method of images.

Kwak [18], Amabili and Kwak [19], Amabili et al. [20] compared natural frequencies obtained by the NAVMI factor solution and the more accurate Rayleigh-Ritz method for rectangular, circular, and annular plates respectively for a situation similar to the Lamb problem. It was found that the fundamental mode and frequency were well estimated by the assumed-modes approach, while higher modes were computed with less accuracy. Tubaldi and Amabili [21] investigated the stability of an infinitely long and wide plate subjected to a pulsating potential flow based on linear dynamics. Tubaldi et al. [22] considered the non-linear dynamic behaviour of the same problem. The flow-induced vibrations of radial and other shell type gates were studied analytically and experimentally in Anami et al. [23,24] and Ishii and Knisely [25]. The coupled hydrodynamic mass and damping were considered for two structural modes, being the streamwise bending of the skin plate and the rotation of the entire gate. Kvalsvold and Faltinsen [26] studied the vibrations of wave slamming against wetdecks of catamaran-type vessels. The wetdeck is modelled as a simply supported bending beam, interacting with the fluid in a two-dimensional domain. The fluid response is determined both analytically and numerically by using the Green's function. The fully coupled gate-fluid problem is subsequently solved by using a fourth order Runge-Kutta integrator. Korobkin and Khabakhpasheva [27] studied a similar problem into more detail including the wetting process and penetration stage based on a modified method of normal modes.

In Tsouvalas and Metrikine [11,28] a semi-analytical model based on linear dynamics is presented to investigate the vibro-acoustic behaviour in offshore pile driving. Due to the high frequencies and water depths involved in this application, the effect of surface waves was omitted. Contrary to many other studies, the fluid problem is solved based on the separation of variables technique. A coupled modal analysis is performed in which the fluid and soil responses are described in terms of in vacuo structural modes. The fluid response therewith becomes an implicit part of the model. The interaction problem between structure and fluid is solved efficiently in this way. Leblond et al. [29] apply a similar approach for the bending of an elastic cylinder, represented as a beam. Three fluid models are considered, namely potential, viscous and acoustic. The modal time dependent displacement coefficients are obtained by matrix inversion in the Laplace domain and fast numerical inversion of the Laplace transform.

Finally, most finite element (FE) packages are able to solve fluid-structure interaction problems for complex geometries. Although developments occur continuously, numerical models including fluid-structure interaction are still computationally expensive and therefore not applied in common engineering practice to test various design parameters and boundary conditions for three dimensional problems [30].

In the present study a model is developed to predict the bending vibrations of a flood gate immersed in fluid. Both fluid compressibility and free surface waves are considered so that the hydrodynamic fluid pressure exerted on the gate is predicted accurately in both low- and high-frequency regimes; this is expected to be relevant for typical flood gates subjected to wave impacts. The approach is similar to Tsouvalas and Metrikine [11] but the effect of free surface waves is added, which is important for the study under consideration. This is the first novel contribution of the paper. The structural and fluid responses are expressed in the frequency domain as a superposition of modes. A semi-analytical solution of the fluid-interaction problem is derived by describing the complete system in terms of in vacuo gate modes. This requires to solve the structure and fluid eigenvalue problems only once for a given geometry and the information can be stored and used subsequently to calculate the response of the system to various load cases. This is a fundamental benefit compared to existing numerical methods. The gate-fluid system is three dimensional, allowing one to study the response to local peak pressures accompanied with wave impacts. In this study, the modal shapes of the gate are based on thin plate theory. However, the method allows for the use of any set of structural modal shapes, which could be obtained by standard FE software for more realistic gate designs.

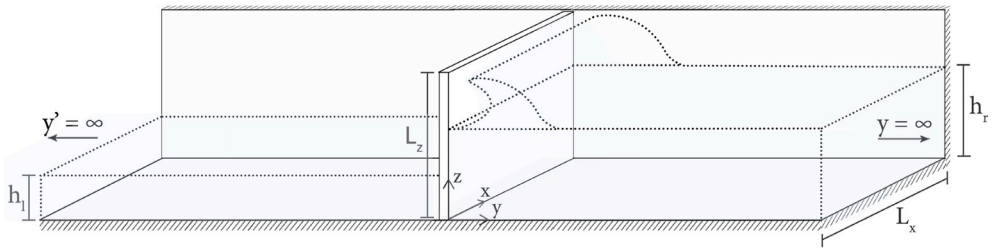

Fig. 1. Three dimensional overview of the plate model space.

The obtained model is able to solve the fluid-interaction for flood gate vibrations computationally efficient and accurately, and is therefore suitable as a preliminary design tool and a large number of simulations. The case study in this paper indicates that this may lead to more economical gate design. Additionally, the model approach allows one to perform fatigue calculations and probabilistic evaluations. The latter is especially interesting as it allows one to study the structural response taking into account the uncertainty associated with wave impacts. This complies to the highly variable nature of wave impacts, as discussed in Hofland et al. [2], in which waves with very similar characteristics lead to significantly different peak pressures. The failure probability of the gate can be quantified explicitly by applying a probabilistic approach based on the developed model, which is valuable for flood safety assessments.

The structure of this paper is as follows. The geometry of the model is described in Section 2. The structure and fluid problem are formulated by linear potential flow and thin plate theory in the time and frequency domains in Section 3. In Section 4, first the structural and fluid modal decomposition is discussed. Subsequently, the fluid-structure interaction problem is tackled. In Section 5 the developed model is applied to a typical case of an impulsive wave impact on a flood gate. The model is validated by comparison with a standard software package in Section 6. Finally, results are discussed in Section 7.

2. Model description

The typical situation of a closed flood gate in a discharge sluice is represented by the model geometry shown in Fig. 1. The sluice has impermeable vertical walls and a horizontal bottom, so that the cross-section of the water body is rectangular. To simplify the analytical derivations, the sluice is assumed to be infinitely long in y-direction. However, cases in which the sluice is of finite dimensions can be treated as well with the adopted modelling approach. The water depths h_l and h_r at the left and right side of the gate respectively, may vary between zero and up to the height of the gate.

The gate structure is represented by a thin plate, that is considered to be homogeneous and isotropic. It is assumed that the contact surface between the structure and fluid is a continuous vertical plane on both sides of the gate. The accuracy of the prediction for more complex gate designs can be improved relatively easily by determining the structural modal shapes with existing FE packages. The developed approach and solution remain identical, as long as the contact surfaces between the gate and fluid are vertical. The aim is to improve suitability of this method for more complex gate geometries and structure-fluid interfaces in further studies.

The gate has a width L_x (equal to that of the sluice), height L_z, distributed mass per unit surface ρ_s, and uniform bending rigidity $D = Et^3/(12(1-\nu^2))$, in which E is the modulus of elasticity, t is the thickness of the gate, and ν is the Poisson's ratio.

The gate is simply supported at its vertical boundaries ($x = 0$, $x = L_x$) and bottom ($z = 0$) while its top edge ($z = L_z$) is stress-free. It is possible to incorporate more complex boundary conditions such as partially clamped in this model as well. In order to keep derivations in this study clear, these relatively simple boundary conditions are chosen without loss of generality.

The fluid system is assumed stationary at both sides with its free surface at h_l and h_r. In the present study a measured breaking wave impact is applied as the excitation force on the gate. The impact pressure is considered to be independent from the gate-fluid system, i.e. the still standing water level is not changed. This assumption is expected to reasonable for wave impacts, as these are typically of much shorter duration (10–100 ms) than the period of the corresponding free surface wave (≈ 10 s) [2]. Furthermore, Cooker and Peregrine [31] developed a mathematical model to predict the wave impact pressure impulse and found it to be only weakly dependent on the shape of the free surface boundary for a similar model geometry. The validity of this assumption is planned to be tested further in experiments in ongoing studies.

3. Theoretical formulation

The governing equations describing the motion of the gate structure and fluid, as defined in previous section, are first introduced. Equations of motions and boundary conditions are presented in the time domain, and subsequently transformed to the frequency domain.

3.1. Structural problem

The linear bending vibrations of a homogeneous isotropic rectangular thin plate are described by the following equation of motion [32]:

$$\rho_s \frac{\partial^2 w(x,z,t)}{\partial t^2} + D\left[\frac{\partial^4 w(x,z,t)}{\partial x^4} + 2\frac{\partial^4 w(x,z,t)}{\partial x^2 \partial z^2} + \frac{\partial^4 w(x,z,t)}{\partial z^4}\right] = -f_l(x, y=0, z, t) + f_r(x, y=0, z, t) + f_e(x, z, t) \tag{1}$$

in which w denotes the displacement of the mid-surface of the plate, ρ_s is the distributed mass per unit of area, f_e the time signal of the external force distribution on the plate (e.g. the wave impact), and f_l and f_r define the fluid pressures at either sides acting on the surface of the gate. As the plate is considered geometrically thin, shear deformation is neglected in Eq. (1). For the cases considered, the wavelengths excited in the structure are large compared to the thickness of the plate which further justifies the choice of the low-order plate theory neglecting high-order effects.

At the simply supported edges the displacement and bending moment in the respective direction are zero. The stress-free top edge of the plate states zero moment and effective Kelvin-Kirchoff shear force in z-direction [33]. The boundary conditions are therefore as follows:

$$w(x=0, z) = M_{xx}(x=0, z) = w(x=L_x, z) = M_{xx}(x=L_x, z) = 0 \tag{2}$$

$$w(x, z=0) = M_{zz}(x, z=0) = M_{zz}(x, z=L_z) = V_{zy}(x, z=L_z) = 0 \tag{3}$$

in which M_{xx} and M_{zz} are the bending moments in x- and z-direction respectively, and V_{zy} is the net shear force in y-direction.

It is assumed that the spatial distribution of the force does not change in time, i.e. the force is separable in a space-dependent part $\hat{f}_{\text{amp}}(x, z)$ and time dependent part $f_t(t)$. Using the Fourier transform pair as stated in Eqs. (4) and (5), transformation to the frequency domain is possible, i.e.:

$$\tilde{G}(\omega) = \int_{-\infty}^{\infty} g(t)\, e^{-i\omega t}\, dt \tag{4}$$

$$g(t) = \frac{1}{2\pi} \int_{-\infty}^{\infty} \tilde{G}(\omega)\, e^{i\omega t}\, d\omega \tag{5}$$

in which $g(t)$ is the examined quantity and $\tilde{G}(\omega)$ its amplitude in the frequency domain, being in this case the displacement of the gate or the fluid pressure. Applying Eqs. (4) and (5) in Eq. (1) yields:

$$-\rho_s \omega^2 \tilde{w}(x,z,\omega) + D\left[\frac{\partial^4 \tilde{w}(x,z,\omega)}{\partial x^4} + 2\frac{\partial^4 \tilde{w}(x,z,\omega)}{\partial x^2 \partial y^2} + \frac{\partial^4 \tilde{w}(x,z,\omega)}{\partial z^2}\right] = -\tilde{f}_l(x, y=0, z, \omega) + \tilde{f}_r(x, y=0, z, \omega) + \tilde{f}_e(x, z, \omega) \tag{6}$$

in which $\tilde{w}$ denotes the complex vibration amplitude of the gate in the frequency domain.

3.2. Fluid problem

The fluid domains at both sides of the plate are mirrored in y-direction. For brevity, the fluid pressure equations are elaborated for a single side of the gate, i.e. $y > 0$, in this and the following section, and the subscripts l or r are omitted.

The fluid is considered irrotational and inviscid. It is to be expected that viscosity plays a negligible role in the dynamic response of the fluid for flood gates. In the wave impact case studied in Section 5 the maximum fluid velocity amplitude is approximately 2 m/s. With a hydraulic radius of the sluice channel of about 4 m this leads to a Reynolds number in the order of 10^6, which is well within the regime where viscous forces are negligible compared to inertial forces.

Based on above consideration the motion of the compressible fluid can be described in terms of the velocity potential ϕ by: The motion of the compressible fluid is described by:

$$\nabla^2 \phi(x,y,z,t) - \frac{1}{c_p^2} \frac{\partial^2 \phi(x,y,z,t)}{\partial t^2} = 0 \tag{7}$$

in which ∇ is the Nabla operator, and c_p is the sound velocity in water. From the dynamic part of the linearised Bernoulli equation for unsteady flow follows the fluid pressure relates to the velocity potential as follows:

$$p(x,y,z,t) = -\rho_f \frac{\partial \phi(x,y,z,t)}{\partial t} \tag{8}$$

The velocity vector of the fluid is given as:

$$v(x,y,z,t) = \nabla \phi(x,y,z,t) \tag{9}$$

The boundary conditions at the impermeable sluice walls and bottom simply state zero velocity. At the still water level of the fluid the free surface condition is applied as known from linear wave theory. At the structure-fluid interface velocity compatibility is inforced. This yields the following set of boundary conditions:

$$\left.\frac{\partial \phi(x,y,z,t)}{\partial x}\right|_{x=0} = \left.\frac{\partial \phi(x,y,z,t)}{\partial x}\right|_{x=L_x} = \left.\frac{\partial \phi(x,y,z,t)}{\partial z}\right|_{z=0} = 0 \tag{10}$$

$$\frac{\partial^2 \phi(x,y,z,t)}{\partial t^2} + g\frac{\partial \phi(x,y,z,t)}{\partial z} = 0 \tag{11}$$

$$\left.\frac{\partial \phi(x, y, z, t)}{\partial y}\right|_{y=0} = \frac{\partial w(x, z, t)}{\partial t} \tag{12}$$

Finally, at $y \to \infty$ the radiation conditions should be satisfied at all times, which completes the statement of the problem. After transformation to the frequency domain Eqs. (7)–(12) become:

$$\nabla^2 \tilde{\phi}(x, y, z, \omega) + k_f^2 \, \tilde{\phi}(x, y, z, \omega) = 0 \tag{13}$$

$$\tilde{p}(x, y, z, \omega) = -\rho_f \, \mathrm{i}\omega \, \tilde{\phi}(x, y, z, \omega) \tag{14}$$

$$\tilde{v}(x, y, z, \omega) = \nabla \tilde{\phi}(x, y, z, \omega) \tag{15}$$

$$\left.\frac{\partial \tilde{\phi}(x, y, z, \omega)}{\partial x}\right|_{x=0} = \left.\frac{\partial \tilde{\phi}(x, y, z, \omega)}{\partial x}\right|_{x=L_x} \left.\frac{\partial \tilde{\phi}(x, y, z, \omega)}{\partial z}\right|_{z=0} = 0 \tag{16}$$

$$\left.\frac{\partial \tilde{\phi}(x, y, z, \omega)}{\partial z}\right|_{z=h} = \frac{\omega^2}{g} \left.\tilde{\phi}(x, y, z, \omega)\right|_{z=h} \tag{17}$$

$$\left.\frac{\partial \tilde{\phi}(x, y, z, \omega)}{\partial y}\right|_{y=0} = i\omega \, \tilde{w}(x, z, \omega) \tag{18}$$

with $k_f^2 = \omega^2 / c_p^2$.

4. Solution to the fluid-structure interaction problem

An analytical solution to the system of equations introduced in previous section is derived by performing a coupled modal analysis. The structural and fluid response are expressed first in terms of modes of vibration. Subsequently, the kinematic condition is satisfied at the structure-fluid interface and the forced system of equations is solved.

This method is aimed at efficiently solving the interaction between structure and fluid. It however remains possible (and in most cases favourable) to evaluate the separate structural and fluid modes and corresponding natural frequencies numerically. In this way, the advantages of existing FE models can be exploited. The fluid equations will be solved completely analytically, since the relatively simple model geometry and separable fluid equation of motion allows for such a treatment in this case. Secondly, from a structural design perspective this is favourable, as it makes possible to quickly evaluate the behaviour of a gate in fluid based on an eigenvalue analysis of the in vacuo gate model in a standard FE package. The modal shapes and natural frequencies of the plate structure are partially found numerically.

4.1. Structural modal expansion

The plate response can be described as the summation of in vacuo modes multiplied by unknown modal amplification:

$$\tilde{w}(x, z) = \sum_{m=1}^{\infty} \sum_{k=1}^{\infty} A_{km} W_{km}(x, z) \tag{19}$$

in which A_{km} are the yet unknown modal amplitudes of each structural mode W_{km}. The modal shapes and corresponding natural frequencies ω_{km} can be found by solving the homogeneous part of Eq. (6) either analytically or numerically. Given the simply-supported boundary conditions along the x-direction in the examined case, a solution can be searched for by applying the separation of variables technique, i.e.:

$$W_{km}(x, z) = W_{x,k}(x) \, W_{z,m}(z) \tag{20}$$

The modal shapes are orthogonal so that the following holds:

$$\iint W_{km} W_{ln} = 0 \quad \text{for } km \neq ln \tag{21}$$

4.2. Fluid modal expansion

The solution to the equation of motion of the fluid, i.e. Eq. (13), can be searched for by applying the separation of variables technique assuming a solution in the following form:

$$\tilde{\phi}(x, y, z) = X(x) \, Y(y) \, Z(z) \tag{22}$$

Substitution into the equation of motion yields three ordinary differential equations including unknown wave numbers k_x, k_y, and k_z for each direction that should fulfill the following condition:

$$k_x^2 + k_y^2 + k_z^2 - k_f^2 = 0 \tag{23}$$

For the considered boundary conditions the following infinite number of modes is found for the x- and z-directions:

$$X_p(x) = \cos(k_{x,p}\, x) \tag{24}$$

$$Z_r(z) = \cos(k_{z,r}\, z) \tag{25}$$

with $p = 1,2, .., \infty$ and $r = 1,2, .., \infty$. The constants are defined by:

$$k_{x,p} = \frac{(p-1)\pi}{L_x} \tag{26}$$

$$\omega^2 = -g k_{z,r} \tan(k_{z,r} h) \tag{27}$$

with h being the water depth at the considered side of the gate. Eq. (27) is known as the surface wave dispersion equation. Solving this equation for a given frequency, yields two imaginary eigenvalues for $k_{z,r}$ (one positive and one negative), and an infinite number of real valued roots.

The solution in y-direction states:

$$Y_p(y) = B_{pr}\, e^{-ik_{y,pr}y} \tag{28}$$

in which B_{pr} are unknown fluid modal coefficients. The separation constants $k_{y,pr}$ are known from Eq. (23):

$$k_{y,pr} = \pm\sqrt{k_f^2 - k_{x,p}^2 - k_{z,r}^2} \tag{29}$$

For $y > 0$, a decaying field representing the evanescent waves along the y-direction holds for $\mathrm{Im}(k_{y,pr}) \leq 0$ while the radiation condition at infinity requires $\mathrm{Re}(k_{y,pr}) \geq 0$. In the ideal case examined here, in which the damping in the fluid region is completely neglected, the latter condition for the propagating modes should always be confirmed by verifying that the group velocity of the waves propagating along the y-direction is positive. This condition is associated with the proper definition of energy propagation towards the positive y-direction carried by the propagating modes in the medium. It can be shown that for the ideal fluid waveguide it is indeed sufficient to consider the poles located on the positive real axis (for $y > 0$). In more complex waveguides, however, i.e. acousto-elastic layered media, this is not aways the case as discussed in van Dalen et al. [34]. Naturally, the inclusion of a small amount of damping will shift the poles to the right half of the complex wavenumber plane making the selection of the proper poles quite straightforward and the need to check the group velocity altogether unnecessary. Thus for the domain $y > 0$ we impose $\mathrm{Re}(k_{y,pr}) \geq 0$ and $\mathrm{Im}(k_{y,pr}) \leq 0$ as shown in Fig. 2.

The representation of the response of the fluid domain in the form of a modal sum over an infinite set of eigenfunctions is exact provided that all poles can be accurately determined in the complex wavenumber plane. Based on complex countour integration and residue theorem it can be shown that for the considered problem this is indeed the case [35].

Combining the modal expansions for the fluid in each direction yields the following expression for $\tilde{\phi}$:

$$\tilde{\phi}(x, y, z) = \sum_{p=1}^{\infty}\sum_{r=1}^{\infty} B_{pr}\cos(k_{z,p}z)\cos(k_{x,r}x)\, e^{-ik_{y,pr}y} = \sum_{p=1}^{\infty}\sum_{r=1}^{\infty} B_{pr}\Phi_{pr}(x, z)\, e^{-ik_{y,pr}y} \tag{30}$$

in which $\Phi_{pr}(x, z)$ are the two-dimensional modal fluid shapes in the plane parallel to the surface of the gate. A similar expression holds for $y < 0$ in which the roots located in the upper half-plane of Fig. 2 need to be considered.

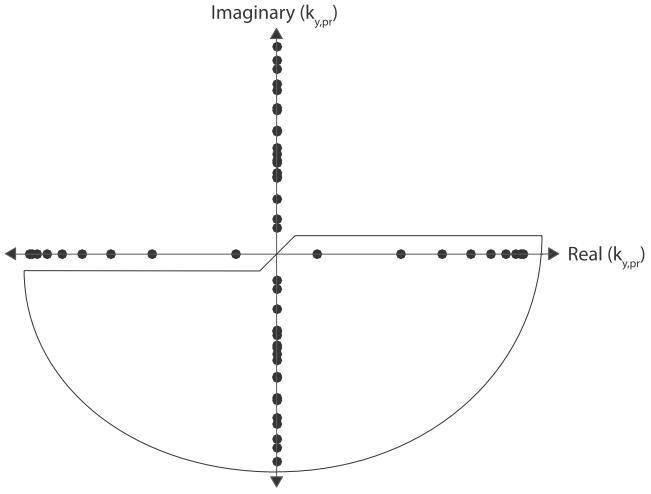

Fig. 2. Contour integration plot for the domain $y > 0$ together with the roots of the dispersion relation for a range of arbitrary parameters.

4.3. Kinematic interface condition between the structure and the fluid

To describe the fluid pressures, excited by the movement of the gate, the solutions for $\tilde{w}$ and ϕ, shown in Eqs. (19) and (30), are substituted into the interface condition of Eq. (18). This yields the following expression:

$$\sum_{p=1}^{\infty}\sum_{r=1}^{\infty} B_{pr}\Phi_{pr}(x,z)\frac{d\left(e^{-ik_{y,pr}y}\right)}{dy}|_{y=0} = i\omega\sum_{m=1}^{\infty}\sum_{k=1}^{\infty} A_{km}W_{km}(x,z) \leftrightarrow -i\sum_{p=1}^{\infty}\sum_{r=1}^{\infty} k_{pr}B_{pr}\Phi_{pr}(x,z) = i\omega\sum_{k=1}^{\infty}\sum_{m=1}^{\infty} A_{km}W_{mk}(x,z) \tag{31}$$

The orthogonality property of the fluid modes yields the following mathematical result:

$$\iint_{S_w}\Phi_{pr}(x,z)\Phi_{qs}\,dx\,dz = \delta_{pq}\delta_{rs}\Delta_{pr}\delta_{pq}\delta_{rs} = \begin{cases}1, & \text{if } p = q \text{ and } r = s\\ 0, & \text{if } p \neq q \text{ or } r \neq s\end{cases} \tag{32}$$

in which S_w is the surface occupied by the stationary fluid at $y = 0$, δ_{pq} and δ_{rs} are Kronecker deltas and Δ_{pr} is the result of the surface integration. Eq. (31) is multiplied by another fluid mode Φ_{qs}, and integrated over the water depth and sluice width to obtain:

$$-\sum_{p=1}^{\infty}\sum_{r=1}^{\infty} k_{pr}B_{pr}\delta_{pq}\delta_{rs}\Delta_{pr} = \omega\sum_{m=1}^{\infty}\sum_{k=1}^{\infty} A_{km}\iint_{S_w} W_{mk}(x,z)\Phi_{pr}(x,z)\,dx\,dz \tag{33}$$

The left-hand side of above equation is non-zero only when $p = q$ and $r = s$. This yields the following expression for B_{pr}:

$$B_{pr} = -\frac{\omega}{k_{pr}\Delta_{pr}}\sum_{k=1}^{\infty}\sum_{m=1}^{\infty} A_{km}Q_{km,pr} \tag{34}$$

with the variable $Q_{km,pr}$ introduced for convenience of notation:

$$Q_{km,pr} = \iint_{S_w} W_{mk}(x,z)\,\Phi_{pr}(x,z)dx\,dz \tag{35}$$

The fluid modal coefficients B_{pr} are now fully described in terms of the structural modal coefficients in a manner similar to Tsouvalas and Metrikine [11]. The coefficients are substituted in the solution for $\tilde{\phi}$ and subsequently in Bernoulli's pressure equation (14). This way the fluid pressure throughout the sluice has been obtained:

$$p_f(x,y,z) = i\omega^2\rho_f\sum_{m=1}^{\infty}\sum_{k=1}^{\infty} A_{mk}\sum_{p=1}^{\infty}\sum_{r=1}^{\infty}\frac{Q_{km,pr}}{k_{y,pr}\Delta_{pr}}\Phi_{pr}(x,z)\,e^{-ik_{y,pr}y} \tag{36}$$

At the surface of the gate (y = 0) the exponential term drops.

From Eq. (36) it can be seen that the real values of $k_{y,pr}$ correspond to the propagating modes and yield an imaginary value of the hydrodynamic pressure in the frequency domain, which is equivalent to radiation damping. The imaginary values of $k_{y,pr}$ correspond to the evanescent modes, i.e. yield real valued hydrodynamic pressures, which either act as a hydrodynamic mass or stiffness depending on the sign. From a physical point of view it is indeed expected that the propagative modes take energy away from the structure.

4.4. Forced system of equations

The solutions for the fluid pressure and structural deflection are now described uniquely in terms of structural modal coefficients. First, the solution of $\tilde{w}(x,z,\omega)$ is substituted in the forced equation (6). For brevity, the function variables are emitted in the remainder of this section with the understanding that all quantities depend naturally on (x,z,ω) at $y = 0$.

$$\sum_{k=1}^{\infty}\sum_{m=1}^{\infty} A_{km}\left[-\rho_s\omega^2\,W_{km} + D\left[\partial^4 W_{km}x + 2\frac{\partial^4 W_{km}}{\partial x^2\partial z^2} + \partial^4 W_{km}z\right]\right] = -\tilde{f}_l + \tilde{f}_r + \tilde{f}_e \tag{37}$$

The structural modes per definition satisfy the homogeneous structural equation of motion. This property is used to eliminate the derivative terms from Eq. (37). Furthermore, the expression in Eq. (36) for the fluid pressure is substituted. This yields the following expression:

$$\sum_{k=1}^{\infty}\sum_{m=1}^{\infty} A_{km}\,\rho_s\,(\omega_{km}^2 - \omega^2)\,W_{km} = -\left[i\omega^2\rho_f\sum_{k=1}^{\infty}\sum_{m=1}^{\infty} A_{km}\sum_{p=1}^{\infty}\sum_{r=1}^{\infty}\frac{Q_{km,pr}}{k_{y,pr}\Delta_{pr}}\Phi_{pr}\right]_{\sum l+r} + \tilde{f}_e \tag{38}$$

in which the subscript $\sum l + r$ denotes the summation of the fluid pressure of left and right side of the gate. Note that, although the analytical expression is identical for both sides, the magnitude of Q_{pr}, k_{pr}, and Φ_{pr} depends on the water depth, and will be different at each side. Due to the orthogonality property of the structural modes the following expression is valid:

$$\iint_{S} W_{km}(x,z)\,W_{ln}(x,z)\,dx\,dz = \delta_{kl}\delta_{mn}\,\Gamma_{ln} \tag{39}$$

in which S denotes the gate surface and Γ_{ln} the solution of the integration. Multiplying Eq. (38) with another structural mode W_{ln} and integrating over the plate surface, yields:

$$\sum_{k=1}^{\infty}\sum_{m=1}^{\infty} A_{km}\,\rho_s\,(\omega_{km}^2-\omega^2)\,\delta_{kl}\delta_{mn}\,\Gamma_{ln} = -\left[\mathrm{i}\omega^2\rho_f\sum_{k=1}^{\infty}\sum_{m=1}^{\infty}A_{km}\sum_{p=1}^{\infty}\sum_{r=1}^{\infty}\frac{Q_{km,pr}\,Q_{ln,pr}}{k_{y,pr}\,\Delta_{pr}}\right]_{\sum l+r} - \iint_S \tilde{f}_e\,W_{ln}\,dx\,dz \tag{40}$$

in which $Q_{ln,pr}$ is defined similar to $Q_{km,pr}$:

$$Q_{ln,pr} = \iint_{S_w}\Phi_{pr}(x,z)\,W_{ln}(x,z)\,dx\,dz \tag{41}$$

4.5. Solution of the gate-fluid motion

An infinite system of analytical equations is now obtained:

$$\sum_{k=1}^{\infty}\sum_{m=1}^{\infty}[\rho_s\,(\omega_{km}^2-\omega^2)\,\delta_{kl}\delta_{mn}\,\Gamma_{ln} - L_{km,ln} + R_{km,ln}]A_{ln} = F_{ln} \tag{42}$$

with the fluid pressures given by:

$$L_{km,ln} = \mathrm{i}\omega^2\rho_f\sum_{p=1}^{\infty}\sum_{r=1}^{\infty}\frac{Q_{km,pr}\,Q_{ln,pr}}{k_{y,pr}\,\Delta_{pr}}|_{h=h_l} \tag{43}$$

$$R_{km,ln} = \mathrm{i}\omega^2\rho_f\sum_{p=1}^{\infty}\sum_{r=1}^{\infty}\frac{Q_{km,pr}\,Q_{ln,pr}}{k_{y,pr}\,\Delta_{pr}}|_{h=h_r} \tag{44}$$

and the modal force given by:

$$F_{ln} = \iint_S \tilde{f}_e(x,z,\omega)\,W_{ln}(x,z)\,dx\,dz \tag{45}$$

Due to the presence of damping, the solutions for $\tilde{w}$ and $\tilde{v}$ from equation (42) will be complex valued. The amplitudes are determined by $|w| = \sqrt{\mathrm{Re}(\tilde{w})^2 + \mathrm{Im}(\tilde{w})^2}$ and $|v| = \sqrt{\mathrm{Re}(\tilde{v})^2 + \mathrm{Im}(\tilde{v})^2}$.

4.6. Stresses in the plate

When the structural deflection field is known, the stress in the isotropic homogeneous plate follows from:

$$\begin{bmatrix}\sigma_{xx}\\ \sigma_{yy}\\ \tau_{xy}\end{bmatrix} = -\frac{Dt_y}{I}\begin{bmatrix}1 & \nu & 0\\ \nu & 1 & 0\\ 0 & 0 & (1-\nu)\end{bmatrix}\begin{bmatrix}\kappa_{xx}\\ \kappa_{zz}\\ \kappa_{xz}\end{bmatrix} \tag{46}$$

with κ_{xx}, κ_{yy} and κ_{zz} being the curvature of the plate in the respective direction.

As a stress criterion Von Mises could be used, which for general plane stress states:

$$\sigma_v = \sqrt{\sigma_{xx}^2 - \sigma_{xx}\sigma_{yy} + \sigma_{yy}^2 + 3\tau_{xy}^2} \le f_y \tag{47}$$

with f_y being the yield strength of the steel material.

4.7. Numerical evaluation of the solution

For evaluation of the system of equation (42), the infinite summations must be truncated to a finite number of structural and fluid modes. The necessary number of modes to provide sufficient accuracy, depends on the excitation frequency in relation to the resonance frequencies of system. A displacement convergence criterion was presented in Tsouvalas et al. [36], which was shown to give a good indication of internal bending moment and shear force convergence as well.

Part of the strength of this semi-analytical method, is that the modal shapes of the structure in vacuo are evaluated only once. Subsequently these modal shapes can be used to evaluate the response at the different excitation frequencies and force amplitude shapes. Due to the inclusion of surface waves in the model, the implicit dispersion equation must be solved for each excitation frequency, which leads to a higher numerical effort compared to the case without surface waves. When evaluating the response for a large number of force frequencies such as is done after a Fourier transformation, in general only a part of the spectrum will result in significant contribution of surface waves.

Any spatial distribution of external forcing can be input to the calculations, as long as only the amplitude and not the distribution is time-dependent. The time-amplitude signal can then be transformed to the frequency domain. An overview of the developed model is shown in Fig. 3. If the force distribution is in fact time-dependent, measures such as a discretization of the external force become necessary. The modal force F_{ln} can be numerically evaluated for each structural mode. Since this part is frequency-independent, a

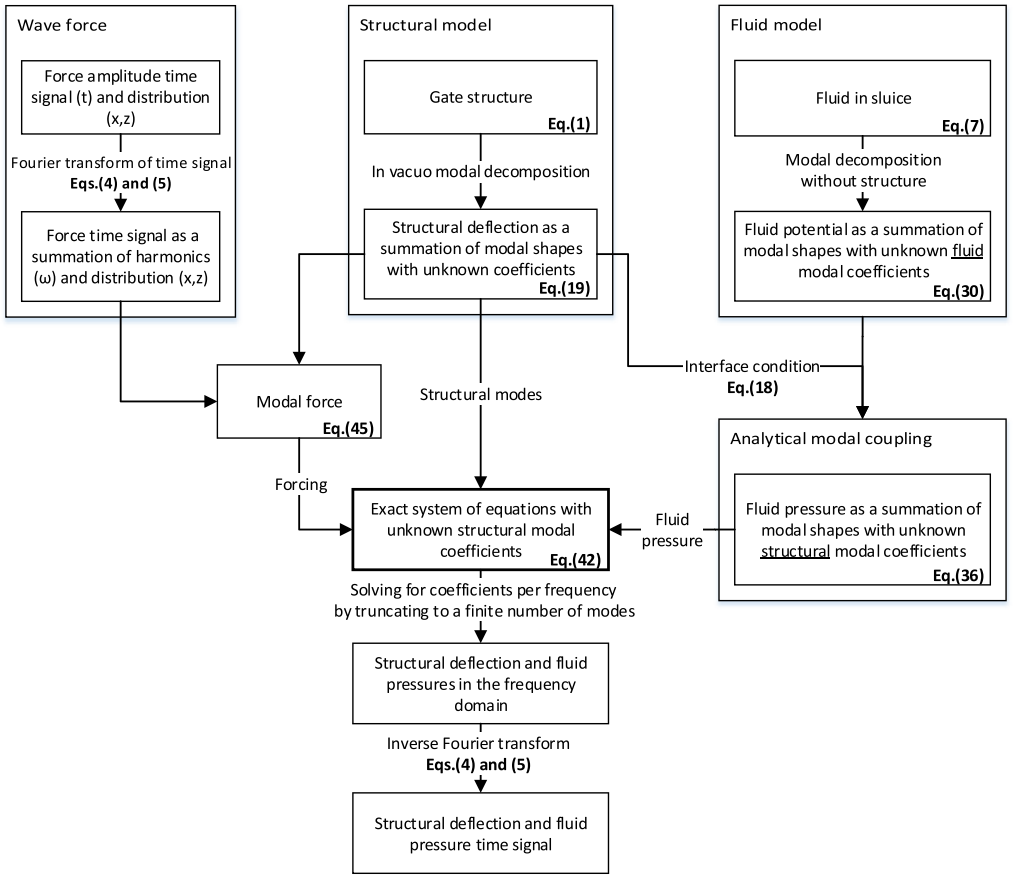

Fig. 3. Overview of the semi-analytical method. The result of the derivations in this chapter is the system of equations in Eq. (42).

single evaluation suffices.

5. Quantitative analysis of a wave impact on a flood gate

The developed model is used to determine the dynamic behaviour of a vertical steel flood gate subjected to a typical wave impact. For this wave impact force full scale pressure measurements are used [2]. The case study is explained in section 5.1 while in section 5.2, the modal expansion of the structure-fluid system is elaborated. Subsequently, in section 5.3 the quasi-static deflection of the gate is determined, and compared to the dynamic time domain response with and without the effect of the surrounding fluid in section 5.4.

5.1. Case study

The system parameters for the case study considered, are shown in Table 1. The gate is maintaining a water level difference of

Table 1
Case parameters and their value.

Structural parameters	Symbol	Value	Unit	Fluid parameters	Symbol	Value	Unit
Width	L_x	12	m	Width	L_x	12	m
Height	L_z	7.5	m	Water level left	h_l	7	m
Gate thickness	t	0.243	m	Water level right	h_r	4	m
Bending stiffness	D	$2.63{\cdot}10^8$	Nm^2	Fluid density	ρ_f	1025	kg/m^3
Distributed mass	ρ_s	95	kg/m^2	Fluid sound velocity	c_p	1500	m/s
Modulus of elasticity (steel)	E	$200{\cdot}10^9$	Nm^2	Gravitational constant	g	9.81	m/s^2
Moment of inertia	I	0.0012	m^4				
Poisson's ratio (steel)	ν	0.3	–				
Yield strength (steel)	f_y	$255{\cdot}10^6$	N/m^2				
Material damping (steel)	η	0.01	–				

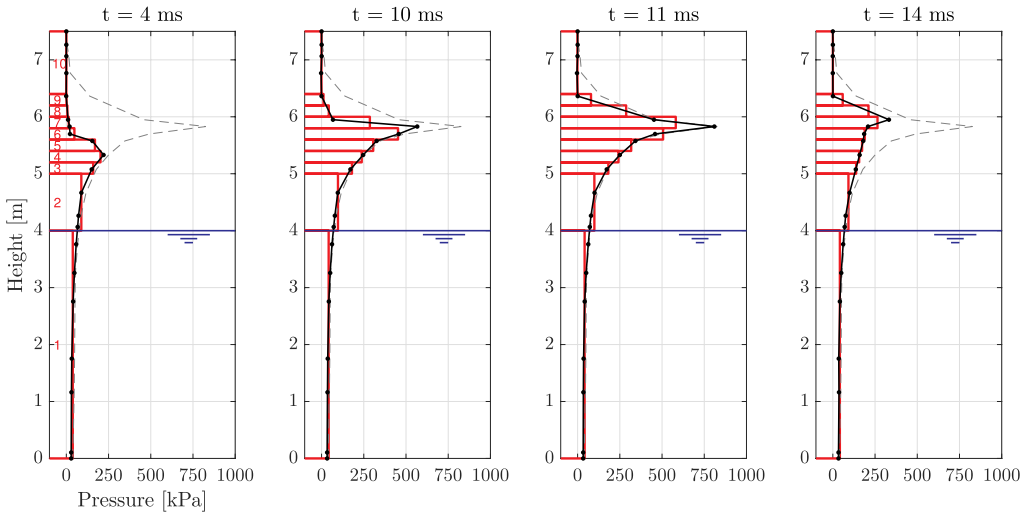

Fig. 4. Wave pressure over the vertical at four moments during impact. The dashed line denotes the envelope of the extreme pressures per location. In red the intervals are denoted that are used as input for the dynamic assessment. (For interpretation of the references to colour in this figure legend, the reader is referred to the Web version of this article.)

3.0 m. The wave impact occurs towards the gate in the $y > 0$ fluid domain, where the lower water level is present. Only the linear dynamic response of the gate as a consequence of the impulsive wave impact force is considered in this study, which needs to be superimposed to the static response due to the presence of the hydrostatic loads at either side of the gate.

The applied wave impact [2, measurement s110,2] is of the flip through type, which is characterised by almost no entrapped air at the time of impact. This type of impact generally involves a large impact force and high peak pressures over short duration, in this case a vertically-integrated maximum force of 707 kN m^{-1} and a maximum pressure of 827 kN m^{-2}. The wave pressure, measured at 19 distinct locations over the vertical coordinate, is depicted for several moments in time during impact in Fig. 4. It can be seen the pressure peak moves upwards during impact. The course of the total impact force per running meter (gate) width in time is shown in Fig. 5 (top).

As the force distribution changes over time, it cannot be separated into a space and time dependent part directly, as required for a direct one-dimensional Fourier transform with respect to time. For this reason, the wave force is divided into ten intervals over the vertical coordinate, which are shown in red in Fig. 4. For every time step, it holds that the vertically-integrated value of the applied pressure is equal to that of the original signal. Each interval will now have its own amplitude-time signal, as shown in Fig. 5 (bottom). The total external force is a summation of the signals in each interval:

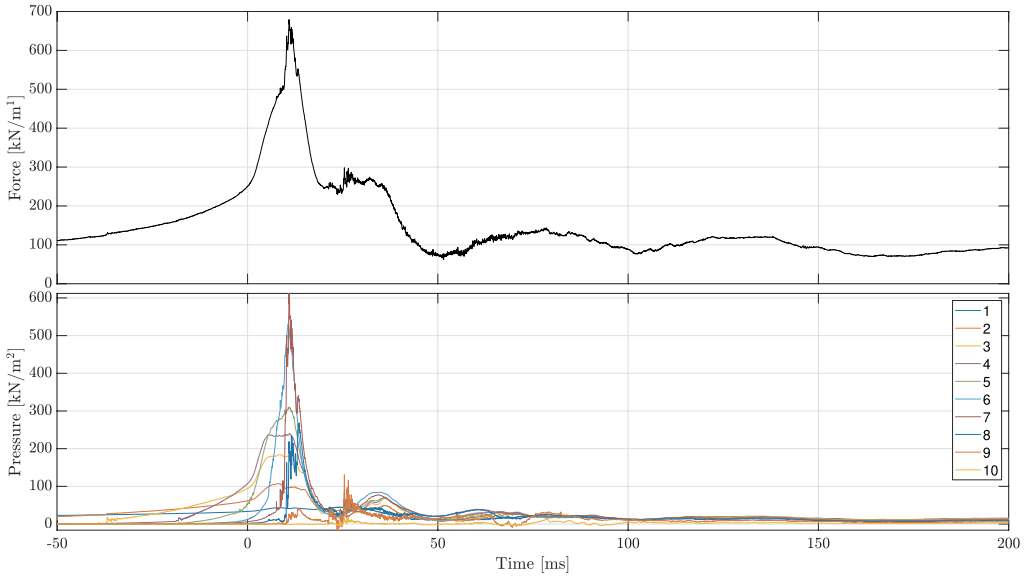

Fig. 5. Vertically integrated wave force and the wave pressure amplitudes for each of the 10 intervals over the vertical of the gate as defined in Fig. 4 over time. The maximum of the integrated wave pressure occurs at $t = 10.88$ ms.

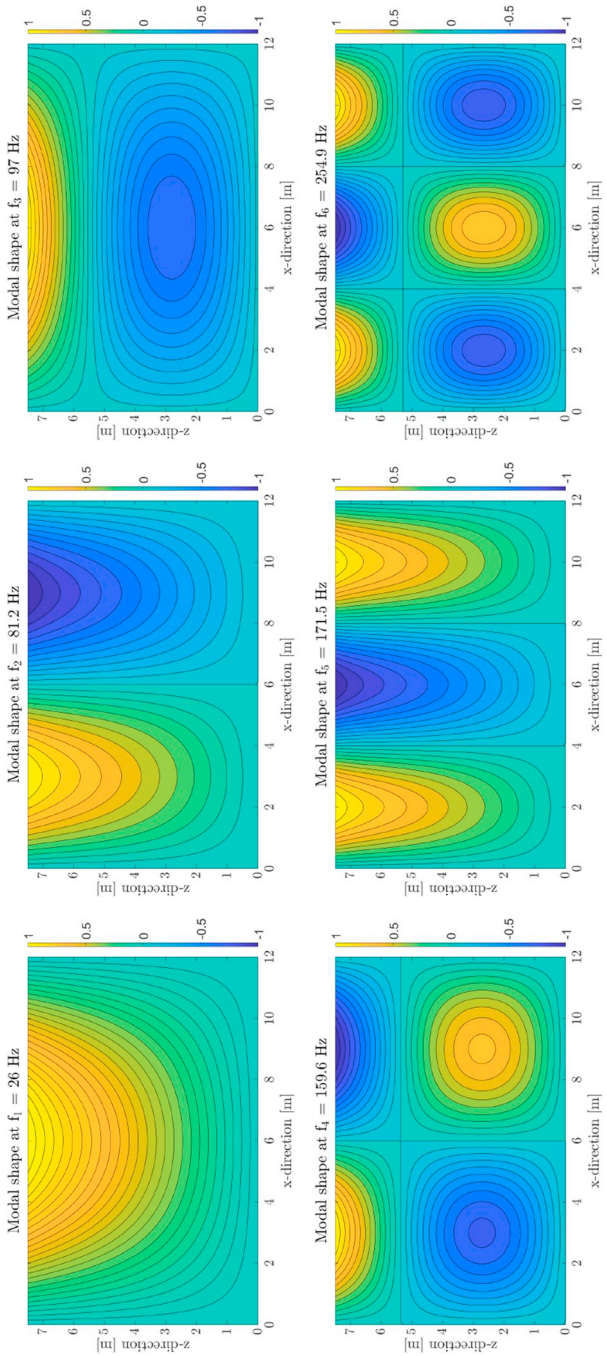

Fig. 6. The in vacuo modal shapes of the gate at the first six natural frequencies.

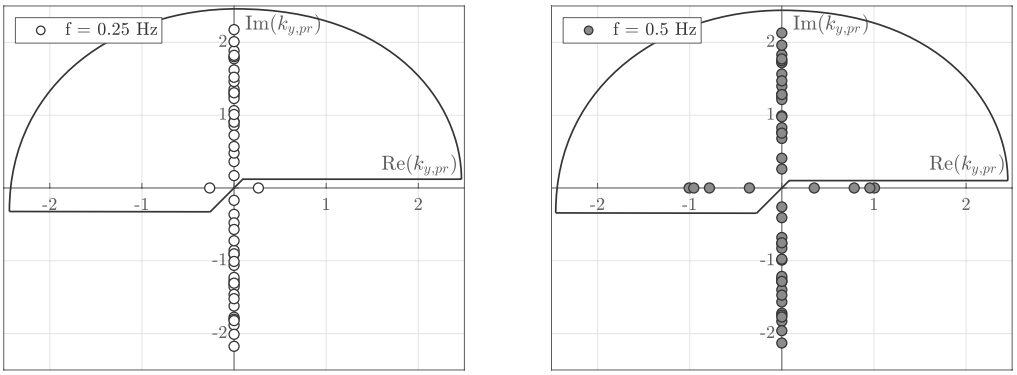

Fig. 7. The first 25 roots $k_{y,pr}$ of the dispersion relation for the fluid domain at $y < 0$ ($h_l = 7$ m) at frequencies 0.25 and 0.5 Hz.

$$f_e(x, z, t) = \sum_{n=1}^{10} [H(z - z_n) - H(z - z_{n+1})] f_{n,t}(t) \tag{48}$$

with f_e being the external wave force, z_n the vertical coordinates that denote the divisions between the intervals, and $f_{n,t}(t)$ the amplitude-time signal for each interval. The error resulting from dividing the force into a certain number of intervals depends mainly on the spatial distribution of the system resonance modes and impact force over the height. For the considered case, the error made by the division of the force into ten intervals was found to be small.

Each signal is Fourier transformed to the frequency domain, and subsequently the plate response is determined. As the model is linear, these responses may be summed. The summed response is transformed back to the time domain, which results in the prediction of the gate response.

5.2. Modal expansion

First, the modal expansion of the gate and fluid will be elaborated for the given system. For simplicity, the material damping η is neglected in the presentation of these results. In Fig. 6 the in vacuo modal shapes of the plate and the corresponding natural frequencies are shown. These have been validated by comparison with the analytical results by Leissa [33]. Since in the studied case the wave impact force has a constant magnitude over the width of the gate, and is therewith symmetric, there will be no response of purely antisymmetric modes to this force. This directly follows from the definition of the modal force in Eq. (45). In the present analysis, the structural and fluid modal expansion are both truncated to the first one hundred modal shapes. For the considered case this was proven to be more than sufficient based on the convergence of the deflection and stresses in the plate as discussed further in Section 5.4.

In Fig. 7 for the fluid domain at $y < 0$ the first 25 roots of the dispersion equation Eq. (29) are depicted for two excitation frequencies. $\mathrm{Re}(k_{y,pr}) \leq 0$ and $\mathrm{Im}(k_{y,pr}) \geq 0$ are imposed for the fluid domain at $y < 0$ to satisfy the radiation conditions as was discussed in section 4.2. The real valued roots $k_{y,pr}$ correspond to propagative fluid modes resulting in hydrodynamic damping, while the imaginary valued roots $k_{y,pr}$ correspond to evanescent modes resulting in hydrodynamic mass and stiffness.

The first six shapes of the submerged structure are shown in Fig. 8. The shape of the submerged gate at the first resonance mode is reasonably similar to the first natural mode of the in vacuo structure as shown in Fig. 6. The vibration shapes at higher resonance frequencies alter substantially. Secondly, the resonance frequencies reduce significantly compared to those of the in vacuo gate, as can be seen in Table 2. Surface waves have a negligible effect on the resonance frequencies as the natural frequencies are relatively high compared to typical frequencies of surface waves at the considered water depths. The effect of surface waves is expected to be greater in the case of a gate-fluid system with lower natural frequencies. The effect of compressibility increases for higher frequencies. The error of considering the fluid as incompressible is limited to approximately 5% for the first 10 resonance frequencies as can be seen from Table 2.

In Fig. 9 the normalised absolute fluid pressure in the fluid domain at $y > 0$ has been depicted for two of the resonance frequencies of the submerged structure. For the fourth resonance frequency, the vibration shape of the gate is clearly recognised. The fluid pressure decays quickly in the direction normal to the surface of the gate. The tenth resonance frequency of the gate-fluid system is close to a natural frequency of the compressible fluid. At the natural fluid frequencies of the fluid, the separation constant $k_{y,pr}$ tends to zero. From Eq. (36), it can be seen that the fluid pressure will then tend to infinity, as $k_{y,pr}$. is in the denominator of the fraction. Secondly, the decay in y-direction tends to diminish as the exponential term $e^{-ik_{y,pr}y} \rightarrow 1$. The shape of the fluid pressure is in this case almost entirely determined by the sluice geometry. For both frequencies shown in Fig. 9, the effect of surface waves on the fluid response has diminished, as the pressure at the still water level is approximately zero.

5.3. Quasi-static response

The quasi-static response of the gate to the wave impact is evaluated with the developed model. The maximum occurring total

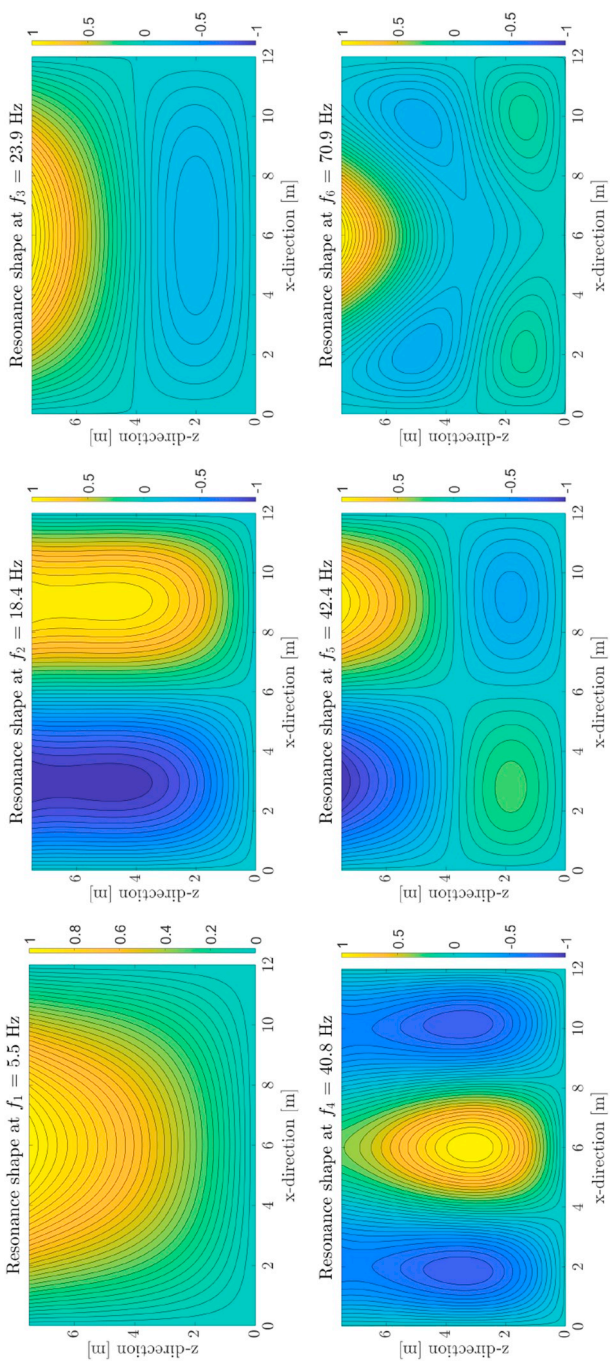

Fig. 8. The amplitude of the complex valued response of gate $\sqrt{\mathrm{Re}^2(w) + \mathrm{Im}^2(w)}$ for the first six resonance frequencies including the effect of the fluid pressure.

Table 2
First ten resonance frequencies of the gate in vacuo and submerged. The resonance frequencies are shown as well for the cases when surfaces waves are excluded or the fluid is considered incompressible.

Condition	f_1	f_2	f_3	f_4	f_5	f_6	f_7	f_8	f_9	f_{10}
In vacuo [Hz]	26.0	81.2	97.0	159.6	171.5	254.9	257.5	297.8	321.1	384.0
Submerged [Hz]	5.5	18.4	23.9	40.8	42.4	70.9	74.6	95.1	114.5	130.6
- Excluding surface waves	5.5	18.4	23.9	40.8	42.4	70.9	74.6	95.1	114.5	130.6
- Incompressible fluid	5.5	18.5	24.1	41.7	43.2	73.8	76.9	100.5	121.1	125.9

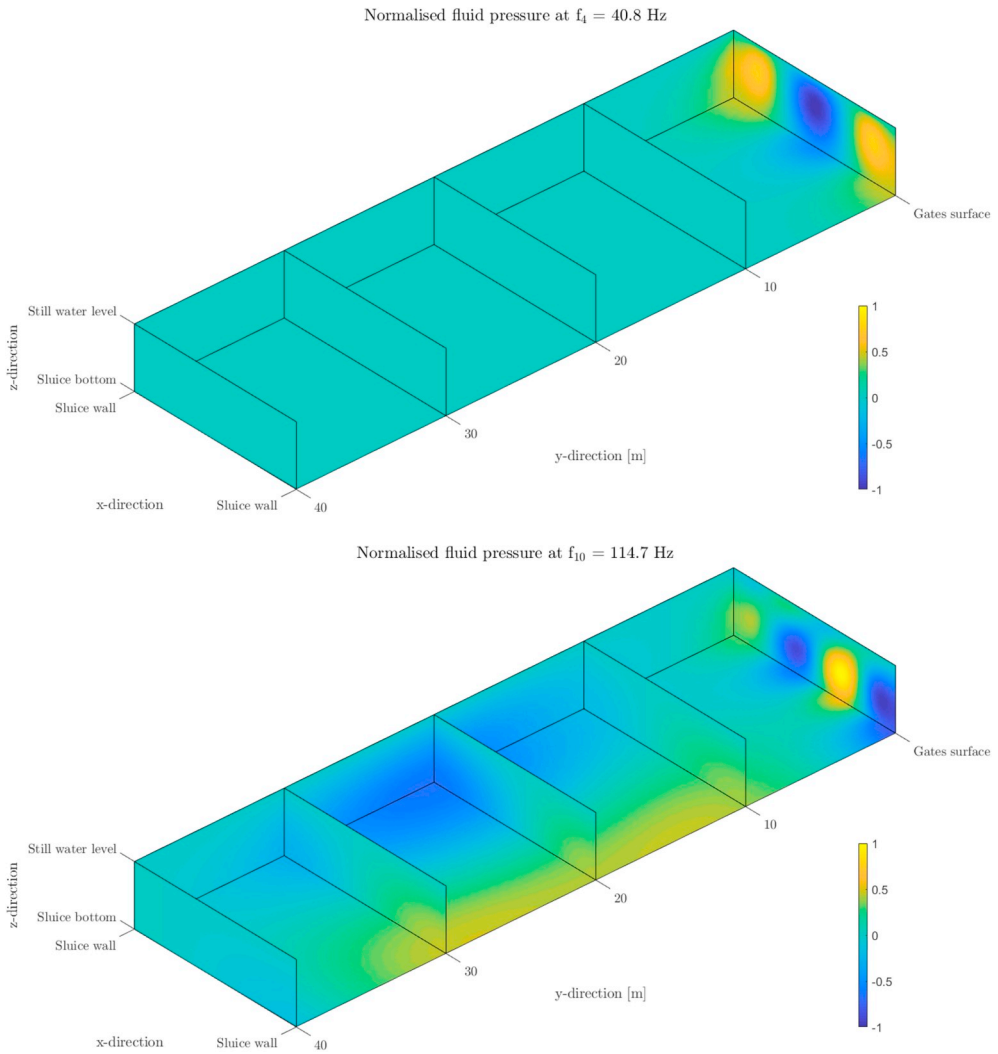

Fig. 9. Normalised absolute fluid pressure throughout the first 40 m of the sluice ($y > 0$) at two of the resonance frequencies of the submerged gate.

wave impact force during the recorded time interval is applied for this purpose. The wave force is divided into ten intervals with equal pressure as defined in Fig. 4 to obtain a valid comparison with the dynamic response. The static behaviour to this force is obtained by setting $\omega = 0$ in Eq. (42). For the quasi-static consideration, the fluid pressure as a consequence of the movement of the gate due to the impact load does not play a role as follows from applying a zero frequency in the expressions for the fluid impedance in Eqs. (43) and (44).

The static response of the gate to the wave impact is depicted in Fig. 10. The maximum deflection of 80.6 mm is found at the middle of the top edge of the gate. This prediction has been validated by a FE model of the plate and results are in good agreement. Stresses and the structural safety are assessed according to the Von Mises yielding stress criterion as presented in Eq. (47). The maximum stress at the surface of the gate is 129 N/mm^2.

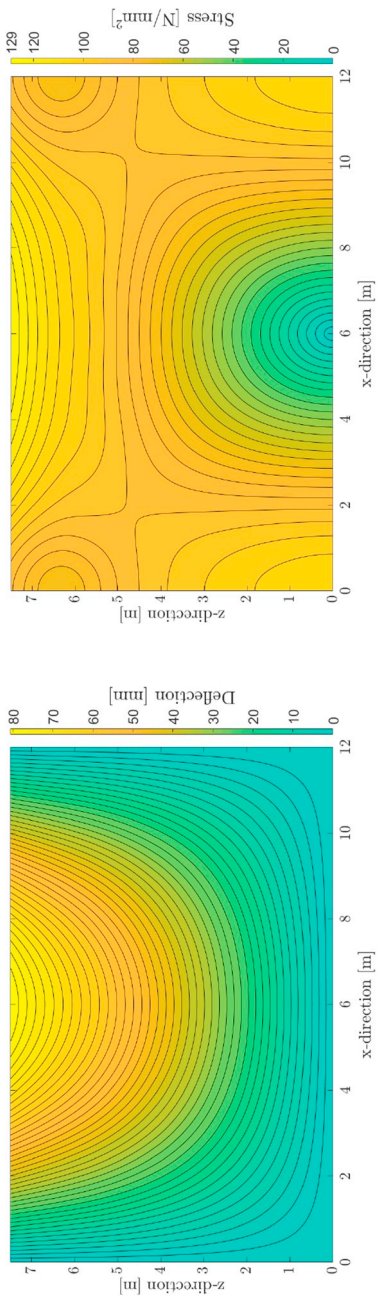

Fig. 10. Quasi-static deflection and stress at the plate's surface due to the maximum wave impact force.

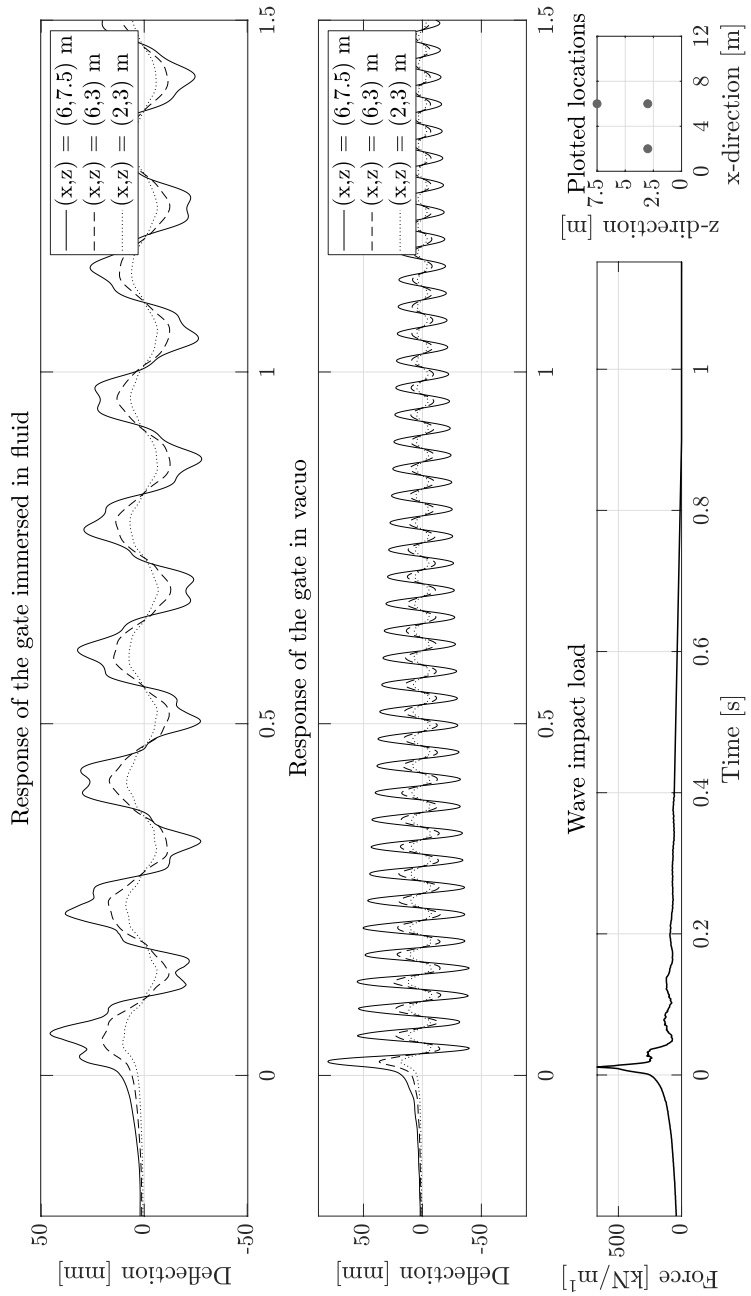

Fig. 11. The dynamic deflection response to the wave impact of several locations of the gate immersed in fluid and in vacuo.

5.4. Dynamic response

As was mentioned in section 5.1, the dynamic response is determined by Fourier transforming each force interval (over the height of the gate) from the time domain to the frequency domain. These frequency domain signals are input to the model and the total deflection is found by the summation of the responses to each of the force intervals. To obtain a stable time signal after application of the inverse Fourier transform, a small amount of material damping is introduced at this point by applying a complex bending stiffness $\tilde{E} = (1 + \eta i)E$ with $\eta = 0.01$ [26]. This type of damping has a minor effect on the natural frequencies of the gate, which herewith become complex.

The displacement of several locations of the gate immersed in fluid during and after impact is shown in Fig. 11. These locations are chosen such that the first three non-asymetric resonance frequencies could be distinguished well. The maximum deflection occurs at the top middle of the gate, and is 45.7 mm. This is significantly lower than the previously determined quasi-static response, which can be explained by the fact that the peak pressure duration ($\approx$ 20 ms) is substantially lower than the first resonance period of the submerged gate ($T_1 = 1/5.5 \approx 182$ ms). Considering the first natural frequency, the system is in fact slow so that the response is not amplified. This is characterised by the deflection of the plate reaching its maximum at $t = 60.0$ ms, while the wave peak pressure occurs at $t = 10.9$ ms. The maximum internal stress is 75.8 N/mm^2.

As a comparison the response of the gate excluding the effect of the hydrodynamic response is shown in Fig. 11 as well. Such analyses have been applied in the design of hydraulic structures before. The maximum deflection would be 80.2 mm, which is close to the maximum static response.

In common engineering practice when a quasi-static modelling approach used, an amplification factor is generally applied to the force to account for possibly unfavourable dynamic behaviour of the structure. Depending on the characteristics of the structure and the type of wave impact, the applied factor varies between 1.0 and 1.5. For the considered case, regarding the dynamic behaviour of the gate immersed in fluid actually lead to a reduction of the maximum stress by almost half of the one obtained with the quasi-static calculation described in section 5.3.

The maximum deflection and internal stress occur at the same time. It is also possible that the maximum internal stress occurs at a different moment in time than the maximum deflection, which can amongst others be a consequence of the excitation of higher structural modes. This is explained by the increase in curvature for higher modal shapes, which leads to larger internal stresses for a given maximum deflection. In Fig. 11 the excitation of higher natural modes can be distinguished as well by the multi-peaked vibration. The deflection at the top middle of the gate, where the maximum occurs, is governed by the first two resonance frequencies.

The results show to be sufficiently converged for the hundred plate and hundred fluid modes taken into account to determine the dynamic response. In Fig. 12 the relative error in the found maximum plate stress is shown in relation to the amount of modes taken into account. When considering higher excitation frequencies a higher number of modes is required to obtain the same level of accuracy. However, this dependence is relatively weak.

6. Validation and computational performance

The performance of the developed semi-analytical model is investigated by comparing its results with the software package

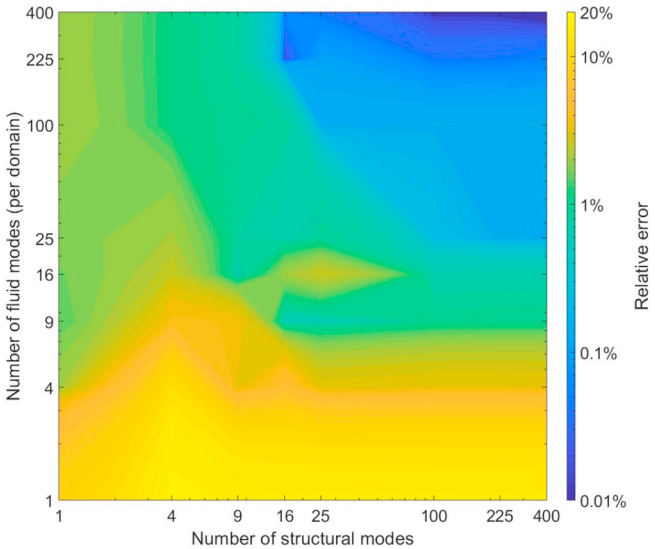

Fig. 12. The error in maximum plate stress found as a function of the number of structural and fluid modes taken into account relative to the result for both four hundred structural and fluid modes.

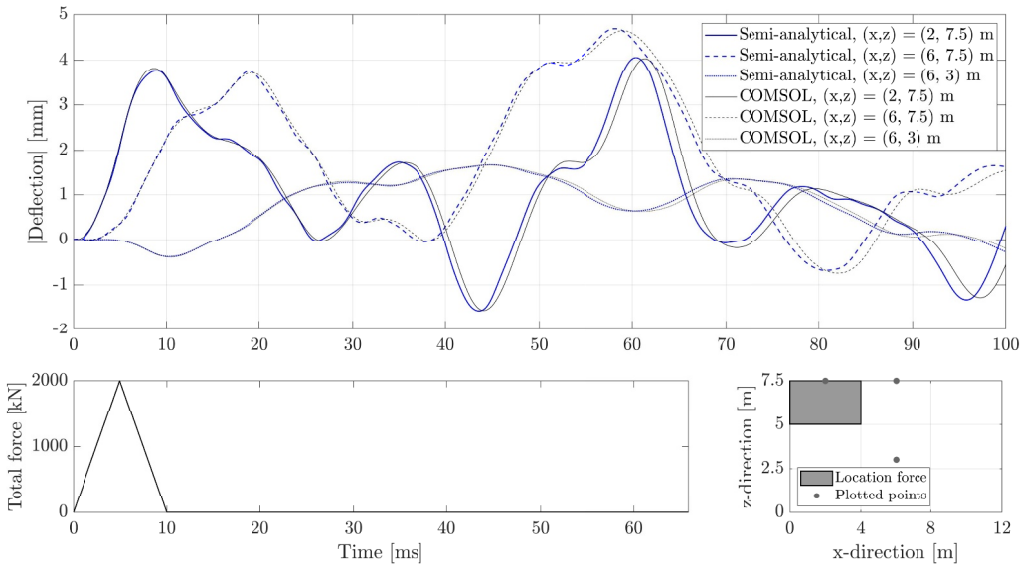

Fig. 13. The time-domain response of the gate immersed in fluid to a triangular peak load predicted by the semi-analytical model and COMSOL.

COMSOL [37]. The same gate-fluid system as described in previous section is investigated. The gate is represented by shell elements (3D) in COMSOL. The material of the gate is considered to be isotropic and linear elastic. The fluid is compressible and modelled with the transient pressure acoustics module of COMSOL. To simplify the COMSOL model surface waves are excluded from the analysis. Instead, a zero pressure boundary condition is applied at the free surface. It has been shown in previous section that this may be assumed for the presented case. The infinite sluice length in y-direction is represented by a standard wave radiation condition at a distance of 100 m from the gate in both fluid domains. For a detailed overview of the shell and transient pressure acoustics theory used in COMSOL is referred to COMSOL Inc [37]. As it is not possible to include material damping in the COMSOL time-domain model, a distributed viscous damping of $c_d = 10$ kNs/m/m^2 is introduced, which acts on the entire surface of the plate.

The results of the wave impact case are not directly compared with the FE model as it is difficult to apply a large number of time-varying force signals at various locations of the gate in the software package COMSOL. Instead, an idealized triangular impact force with a duration of 10 ms is applied on the left upper part of the gate. Such an impact force of short duration is especially suitable for the purpose of validation, as it ensures a wideband frequency spectrum that excites multiple system modes. The same numerical routine is used to obtain the results for the validation study as for the wave impact case.

A variable triangular mesh is used for the shell and a variable tetrahedral mesh for the fluid domain. Both have a maximum element size of 1 m. The time-domain results converge for this element size.

The time domain results of both models are shown for multiple locations on the gate in Fig. 13. As can be seen, the results match closely even though minor differences in predicted frequencies of the response cumulate over time. A comparison of the resonance frequencies predicted by both models is shown in Table 3. The relatively small differences in the resonance frequencies for the in vacuo plate are expected to be caused by the omission of shear deformation in the semi-analytical model. As expected, this error increases for higher modes. The difference between predicted resonance frequencies for the immersed condition is in the same order. This is expected to partially originate from the COMSOL model as results showed some dependency on mesh size and sluice length for eigenfrequency analysis, which did not converge within the range that could be investigated with reasonable computation times.

The computation time of the semi-analytical model for the presented time-domain analysis took 12 min on a 3.60 GHz quad core processor, while computation with the COMSOL model lasted approximately 19.5 h. The computational efficiency of the semi-analytical code has not been fully optimised yet and can still be improved. Furthermore, the response of the same system can be investigated for a range of loads with relatively little additional computation time.

Table 3
Comparison of the first five predicted resonance frequency between the semi-analytical and COMSOL model for the in vacuo and immersed system.

Condition	Model	f_1	f_2	f_3	f_4	f_5
In vacuo	Semi-analytical [Hz]	26.05	81.15	96.97	159.61	171.49
	COMSOL [Hz]	25.93	80.43	95.78	156.60	168.69
	Relative difference [−]	0.46%	0.90%	1.24%	1.92%	1.66%
Immersed	Semi-analytical [Hz]	5.51	18.36	23.89	40.81	42.39
	COMSOL [Hz]	5.49	18.14	23.52	40.39	41.50
	Relative difference [−]	0.36%	1.21%	1.57%	1.04%	2.14%

It must be noted that the superposition of modal responses is valid only for a linear system. Any non-linearities are therefore omitted. For highly non-linear interaction problems, it therefore remains necessary to resort to the more computationally intensive coupled numerical time domain methods. For many hydraulic engineering cases however, the presented method is expected to represent the behaviour with sufficient accuracy at least for preliminary design stages. For flood defence structures in the Netherlands especially the linear elastic behaviour of the material is relevant, as these structures must be designed based on a non-plastic stress criterion.

7. Conclusion

A semi-analytical model has been developed that allows to study the bending vibrations of a gate immersed in fluid subjected to any time varying force. The developed method accounts for the three dimensional behaviour of both the structure and fluid, and solves the involved interaction efficiently. It is important to mention that one needs to solve the structure and fluid eigenvalue problems only once for a given geometry and water heights. The values can be stored and used to calculate the response to any given impact load. This is a fundamental difference compared to standard numerical methods. The adopted method does not depend on the assumed-modes approach. Furthermore, surface waves and compressibility were taken into account so that the hydrodynamic fluid pressure exerted on the gate is predicted accurately in both low and high frequency regimes. Due to the method's computational efficiency and accurate representation of the problem, it can be applied efficiently as a preliminary design tool. This is a step forward from the single or two degree of freedom models used often in present design practice, which give no continuous information on the deflection and internal stresses along the gate or in the fluid domain. Additionally, the model allows to perform fatigue calculations and probabilistic assessments. Results of the developed model were compared against the ones obtained with FEM simulations for the case of an idealized triangular pressure pulse applied on the gate. It is demonstrated that the computational method adopted in the former is capable of providing results similar to those of a detailed FE model within a fraction of the computation time of the latter.

A measured wave impact signal was applied to a flood gate design as a case study. As expected the prediction of the dynamic response, including the interaction between the gate and the surrounding fluid system, lead to a significantly different assessment of the safety than based on the static response only. In the considered problem, the consideration of the dynamic behaviour and the fluid-structure interaction resulted in a more economical design. This illustrates that considering the dynamic behaviour in gate design, rather than using a quasi-static approach with a conservative amplification factor (usually a 50% increase of the maximum force), can have economical advantages as well next to the more accurate determination of the expected dynamic behaviour.

Surface waves did not significantly influence the hydrodynamic response of the gate for the excitation and resonance frequencies that were involved in the breaking wave impact case study. Compressibility mainly had an effect on the higher resonance frequencies of the gate-fluid system. For the studied gate, which was considered homogeneous and isotropic, the first two system resonance frequencies governed its response. Considering more realistic and detailed gate designs consisting of beams and plates, and varying design impacts for certain parts of these gates, is expected to further increase the importance of taking higher vibration modes into account.

Declarations of interest

None.

Acknowledgements

This research was supported by Rijkswaterstaat (contract RWT31120028) and NWO grant ALWTW.2016.041.

References

[1] Ramkema C. A model law for wave impacts on coastal structures. Coast. Eng. Proc. 1978;16:2308–27.
[2] Hofland B, Kaminski M, Wolters G. Large scale wave impacts on a vertical wall. Coast. Eng. Proc. 2011;1:15.
[3] Bagnold RA. Interim report on wave-pressure research Technical Report 7 Institution of Civil Engineers; 1939. https://doi.org/10.1680/ijoti.1939.14539http://www.icevirtuallibrary.com/doi/10.1680/ijoti.1939.14539.
[4] Lamb H. On the vibrations of an elastic plate in contact with water. Proc R Soc Lond - Ser A Contain Pap a Math Phys Character 1921;98:205–16.
[5] Kolkman PA, Jongeling THG. Dynamic behaviour of hydraulic structures - Part B. 2007.
[6] Cuomo G. Wave impacts on vertical seawalls and caisson breakwaters, PIANC magazine "on course" 127. 2007.
[7] Hattori M, Tsujioka N. Dynamic Response of vertical elastic walls to breaking wave impact. Coast Eng 1996;1997:2456–69. https://doi.org/10.1061/9780784402429.190.
[8] Goda Y. Random seas and design of maritime structures vol. 15. World Scientific Publishing Co. Pte. Ltd; 2000. p. 1–462.
[9] Technische Adviescommissie voor de Waterkeringen, Kunstwerken Leidraad. Technical report. 2003.
[10] US army corps of engineers. Coastal Engineering Manual. 2002. Engineer manual 1110–2-1100.
[11] Tsouvalas A, Metrikine A. A semi-analytical model for the prediction of underwater noise from offshore pile driving. J Sound Vib 2013;332:3232–57.
[12] Kolkman PA, Jongeling THG. Dynamic behaviour of hydraulic structures - Part A. 2007.
[13] Kwak MK, Kim KC. Axisymmetric vibration of circular plates in contact with fluid. J Sound Vib 1991;146:381–9.
[14] Kolkman P. A simple scheme for calculating the added mass of hydraulic gates. J Fluid Struct 1988;2:339–53.
[15] Westergaard HM. Water pressure on dams during earthquaks. Trans Am Soc Civ Eng 1933;95:418–33.
[16] Fu Y, Price WG. Interactions between a partially or totally immersed vibrating cantilever plate and the surrounding fluid. J Sound Vib 1987;118:495–513.
[17] Ergin A, Ugurlu B. Linear vibration analysis of cantilever plates partially submerged in fluid. J Fluid Struct 2003;17:927–39.
[18] Kwak MK. Hydroelastic vibration of rectangular plates. J Appl Mech 1996;63:110.

[19] Amabili M, Kwak MK. Free vibrations of circular plates coupled with liquids: revising the lamb problem. J Fluid Struct 1996;10:743–61.
[20] Amabili M, Frosali G, Kwak MK. Free vibrations of annular plates coupled with fluids. J Sound Vib 1996;191:825–46.
[21] Tubaldi E, Amabili M. Vibrations and stability of a periodically supported rectangular plate immersed in axial flow. J Fluid Struct 2013;39:391–407.
[22] Tubaldi E, Amabili M, Alijani F. Nonlinear vibrations of plates in axial pulsating flow. J Fluid Struct 2015;56:33–55.
[23] Anami K, Ishii N, Knisely C. Field vibration tests and dynamic stability analysis of a full-scaled tainter-gate. American society of mechanical engineers, pressure vessels and piping division, vol. 488. (Publication) PVP; 2004. p. 81–8. https://doi.org/10.1115/PVP2004-3008.
[24] Anami K, Ishii N, Knisely CW. Added mass and wave radiation damping for flow-induced rotational vibrations of skinplates of hydraulic gates. J Fluid Struct 2012;35:213–28.
[25] Ishii N. Knisely, Flow-induced vibration of shell-type long-span gates. J Fluid Struct 1992:681–703.
[26] Kvalsvold O M Faltinsen. Hydroelastic modelling of slamming against wetdecks. 8th international workshop on water waves and floating bodies. 1993. p. 57–60.
[27] Korobkin AA, Khabakhpasheva TI. Regular wave impact onto an elastic plate. J Eng Math 2006;55:127–45.
[28] Tsouvalas A, Metrikine A. A three-dimensional vibroacoustic model for the prediction of underwater noise from offshore pile driving. J Sound Vib 2014;333:2283–311.
[29] Leblond C, Sigrist J, Auvity B, Peerhossaini H. A semi-analytical approach to the study of an elastic circular cylinder confined in a cylindrical fluid domain subjected to small-amplitude transient motions. J Fluid Struct 2009;25:134–54.
[30] Erdbrink CD. Modelling flow-induced vibrations of gates in hydraulic structures PhD. thesis University of Amsterdam; 2014.
[31] Cooker MJ, Peregrine DH. Pressure-impulse theory for liquid impact problems. J Fluid Mech 1995;297:193–214.
[32] Clausen WE, Hopper AT, Hulbert LE, Leissa AW. A comparison of approximate methods for the solution of plate bending problems. AIAA J 1969;7:920–8.
[33] Leissa AW. Vibration of plates. 1969. Washington, D.C.
[34] van Dalen KN, Tsouvalas A, Metrikine AV, Hoving JS. Transition radiation excited by a surface load that moves over the interface of two elastic layers. Int J Solid Struct 2015;73–74:99–112.
[35] Tsouvalas A. Underwater noise generated by offshore pile driving Ph.D. thesis Delft University of Technology; 2015. https://doi.org/10.4233/uuid:55776f60-bbf4-443c-acb6-be1005559a98.
[36] Tsouvalas A, van Dalen KN, Metrikine AV. The significance of the evanescent spectrum in structure-waveguide interaction problems. J Acoust Soc Am 2015;138:2574–88.
[37] COMSOL Inc. COMSOL multiphysics reference manual, version 5.3 Technical Report 2018www.comsol.com.